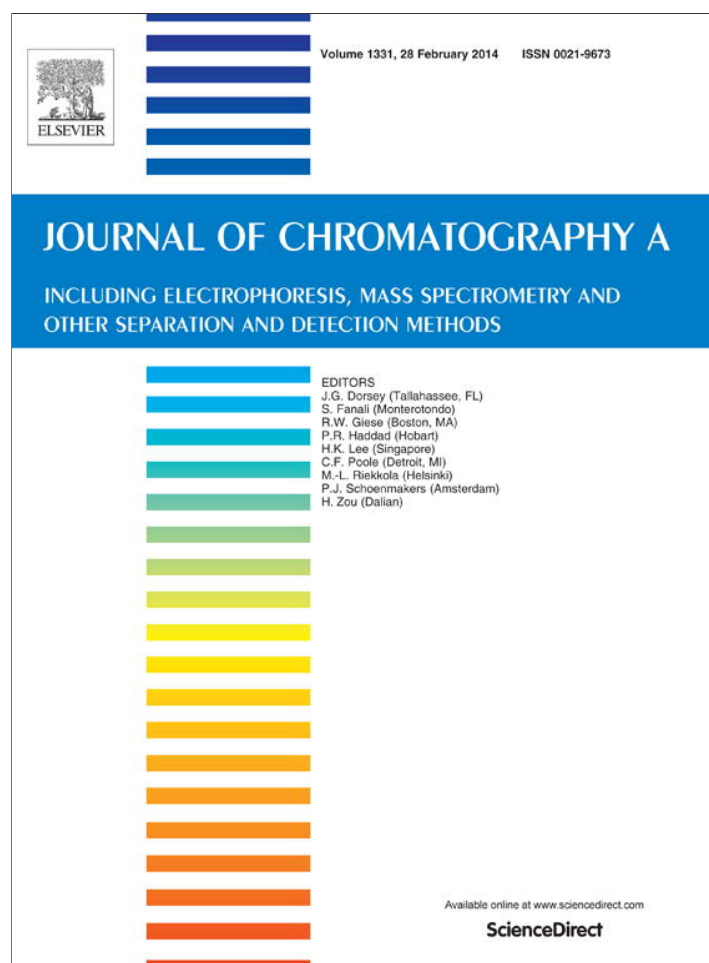


Provided for non-commercial research and education use.
Not for reproduction, distribution or commercial use.



This article appeared in a journal published by Elsevier. The attached copy is furnished to the author for internal non-commercial research and education use, including for instruction at the authors institution and sharing with colleagues.

Other uses, including reproduction and distribution, or selling or licensing copies, or posting to personal, institutional or third party websites are prohibited.

In most cases authors are permitted to post their version of the article (e.g. in Word or Tex form) to their personal website or institutional repository. Authors requiring further information regarding Elsevier's archiving and manuscript policies are encouraged to visit:

<http://www.elsevier.com/authorsrights>



Contents lists available at ScienceDirect

Journal of Chromatography A

journal homepage: www.elsevier.com/locate/chroma

Electromigration behavior of nucleic acids in capillary electrophoresis under pulsed-field conditions

Zhenqing Li^{a,b}, Chenchen Liu^a, Xiaoming Dou^{a,b,*}, Yi Ni^a,
Jiaxuan Wang^a, Yoshinori Yamaguchi^{c,b,a}^a Engineering Research Center of Optical Instrument and System, Ministry of Education, Shanghai Key Lab of Modern Optical System, University of Shanghai for Science and Technology, No. 516 Jungong Road, Shanghai 200093, China^b Institute for Biomedical Engineering, Consolidated Research Institute for Advanced Science and Medical Care (ASMeW), Waseda University, 513 Wasedatsurumaki-cho, Shinjuku-ku, Tokyo 162-0041, Japan^c Photonics Advanced Research Center, Graduate School of Engineering, Osaka University, Yamadaoka Suita-city, Osaka 565-0871, Japan

ARTICLE INFO

Article history:

Received 19 May 2013

Received in revised form

11 November 2013

Accepted 10 January 2014

Available online 15 January 2014

Keywords:

DNA/RNA/Pulsed field capillary electrophoresis/urea/acetic acid

ABSTRACT

We have presented a study focused on the migration pattern of double-stranded DNA (dsDNA) and RNA under pulsed field conditions. By calculating the dependence of nucleic acid mobility on its molecular size in a double logarithm plot, we found that (I) dsDNA molecules proceeded by a sigmoidal migration regime which was probably related to Ogston sieving, transition regime, and reptation model. Furthermore, the transition regime disappeared if DNA was resolved in a higher molecular mass HEC. (II) The migration pattern of RNA was relevant to the denaturant used for separation. When RNA was denatured by acetic acid, its mobility parabolically declined with its molecular size. The mobility was linearly decreased with the molecular size if urea was employed as denaturant. (III) RNA may migrate by Ogston, reptation without orientation mechanism when denatured by urea, whereas these two models were not suitable for RNA if denatured by acetic acid. Even though the electrophoretic conditions of PFCE were varied, the sigmoidal, linear, parabolic migration patterns could still be observed. (IV) Under certain modulation depth, the migration time (T_m) of acetic acid decreased with the increase of average separation voltage (V_a), and when RNA denatured in 4.0 M urea, T_m showed a linear correlation with V_a . (V) The mobility of nucleic acids increased with the growth of artificial temperature in the capillary volume due to the decrease in the viscosity of the polymer. This is the first systematic and comparative research of high molecular mass nucleic acids in PFCE, which provides us deep insight into RNA and DNA migration behavior under pulsed electric field conditions.

© 2014 Elsevier B.V. All rights reserved.

1. Introduction

Capillary electrophoresis (CE) has been recognized as an attractive separation method because of its numerous advantages (e.g., low sample and electrolyte consumption, short analysis time, and high efficiency). Therefore, nucleic acid analysis by CE is now a powerful tool in many research fields, including polymerase chain reaction product analysis, DNA restriction fragments analysis, DNA fingerprinting and DNA sequencing [1–5]. However, at strong electric fields and/or large molecular weight, the velocity of an oriented DNA chains will segregate in aggregates, and thus DNA molecules of different size cannot be separated by direct current (DC) field CE [6,7,8]. For the first time, Carle et al. improved resolution between large DNA molecules by alternating fields in gel electrophoresis [9]. This technique was then used to confer size-dependent mobility by

periodically changing the direction and magnitude of the applied field, essentially relaxing molecular elongation [10–12]. After that, Cohen and Karger further applied pulsed electric field to CE [13].

In pulsed field capillary electrophoresis (PFCE), the reorientation time of the DNA molecule is determined by the polymer concentration in background electrolyte, pulse frequency (time duration for the forward t_f and backward t_b), modulation depth (the separation voltage for the forward V_f and backward V_b), and DNA molecular size. They are the global electrophoretic parameters for DNA separations in PFCE. Our previous experiments showed that in square-wave PFCE ($t_f = t_b$, $V_f \neq V_b$), small DNA fragments were better separated with low polymer concentration and modulation depth, whereas larger fragments were better resolved with high polymer concentration and modulation depth [14]. Further research showed that in inversion field CE ($t_f \neq t_b$, $V_f = V_b$), both short and long DNA fragments could be simultaneously separated with high resolution [15]. Traditionally, RNA needs to be denatured to cleave the hydrogen bond in the secondary and tertiary structures prior to CE or slab gel electrophoresis. By adding acetic acid

* Corresponding author. Tel.: +86 21 55276023; fax: +86 21 55276023.

E-mail addresses: zhenqingli@163.com (Z. Li), xiaomingdou@yeah.net (X. Dou).

into the polymer, we developed an on-line PFCE technology to realize denaturing and separating RNA simultaneously in a capillary [16]. We have also analyzed the separation performance of RNA between 0.1 and 10.0 knt (kilo nucleotide) by PFCE with 4.0 M urea as denaturant [17].

The migration mechanisms of single and double strand DNA (dsDNA) in traditional constant field CE have been extensively studied in the past few years [18–21]. In semi-dilute solutions, Ogston model, reptation model, and their improved version were developed for the description of DNA movements in gels and polymer solution [19,22]. For short DNA with radius of gyration ($R_{g,DNA}$) smaller than the pore size (ξ_b), separation was deemed to relate to the classical Ogston sieving [23]. This theory assumed that the gel acted as a sieve with a distribution of pore sizes and the separation was regarded as a kind of filtration, driven by the electric field. For larger nucleic acids with $R_{g,DNA} > \xi_b$, the migration was supposed to proceed by reptation or segmental motion [24], in which the DNA was supposed to migrate in a snake-like fashion through a “tube” defined by the fibers (for a rigid mesh) or the “blobs” (for a flexible network) surrounding it. However, although PFCE was widely utilized for the separation of large DNA fragments, so far no research has yet been carried out on a detailed description of the migration mechanisms of nucleic acids under pulsed field conditions.

The relationship between nucleic acid size and its mobility exposes the migration behavior of RNA/DNA in the polymer, and this relationship is a key to optimize the separation and quantify the individual components in a mixture. Herein, for the first time, we present a systematic and detailed study on the motion of nucleic acids in hydroxyethyl cellulose (HEC) under pulsed field conditions. The main electrophoretic factors for PFCE were varied and the results were compared with existing electrophoresis theories in CE. In order to cleave the hydrogen bond in the secondary and tertiary structures, RNA was denatured by urea and acetic acid, respectively. Such a study is beneficial in elucidating nucleic acids migration information and achieving an optimal RNA/DNA separation conditions in PFCE.

2. Materials and methods

2.1. Chemicals

0.1 kbp (kilo base pairs) and 1.0 kbp- DNA ladders were purchased from Takara (Shiga, Japan). 0.1 and 0.2 knt- Perfect RNATM Markers were received from Novagen (San Diego, USA). HEC with sizes of 250 k and 1300 k was bought from Polysciences (Warrington, PA, USA). Urea and acetic acid were obtained from Wako Pure Chemical Industries (Osaka, Japan). 10,000 × SYBR Green I and II were got from Invitrogen (Carlsbad, CA, USA). 10 × TBE (1 × TBE = 89 mM Tris/89 mM boric acid/2 mM EDTA, pH 8.4) buffer was bought from Bio-Rad (Hercules, CA, USA). 0.5 × TBE was prepared by mixing 10 × TBE and distilled water with a ratio 1:19, fluorescence dye (1 × SYBR Green I for DNA separation, 1 × SYBR Green II for RNA separation denatured by urea and 3 × SYBR Green II RNA separation denatured by acetic acid, respectively). 1 × or 3 × SYBR Green I/II was obtained by diluting the 10,000 × SYBR Green I/II to a final concentration of 1/10,000 or 3/10,000, respectively.

2.2. Pulsed-field capillary electrophoresis

A home-built PFCE system was described elsewhere [17]. The fused-silica capillaries (15 cm total length; 8 cm effective length; 75 μm i.d.; 365 μm o.d.) were purchased from Polymicro Technologies (Phoenix, AZ, USA). The capillaries were coated with polyacrylamide to suppress the electroosmotic flow [25,26]. The excitation wavelength from a mercury lamp was filtered

to be 460–495 nm, which was the wavelength of the excitation maximum of the conjugate of SYBR Green II and the nucleic acid. The fluorescence emission was collected by a 60 × objective (PlanApo/IR, Olympus), and then was monitored by a photomultiplier tube (R928, Hamamatsu Photonics, Japan). A high-voltage power supply (MODEL 610E, TREK, Medina, NY, USA) was employed to drive the electrophoresis. The applied voltage and data collection were controlled by LabVIEW software (National Instrument, Austin, TX, USA). The entire detection system was enclosed in a dark box. Samples were electrokinetically introduced into the capillary. After each electro-separation, the capillary was flushed with sterilized water by pump (2XZ-1, Hede Laboratory Equipment Co., Ltd., Shanghai, China) for 1.0 min, and the air exhaust rate was 60 l per s. The viscosity of the HEC solution was measured by SNB-1 viscometer (Nirun Intelligent Technology Co., Ltd., Shanghai, China). All separations were performed at 26 °C in the super clean room controlled by central air conditioning.

3. Results and discussion

3.1. Nucleic acid separation

A series of experiments about dsDNA and RNA separation in semi-dilute polymer solutions were performed under different PFCE conditions, including polymer concentration, modulation depth and pulse frequency. Fig. 1 shows an example of electropherogram of nucleic acids separations in 0.5 × TBE buffer containing 0.5% HEC (250 k) with square-wave PFCE (100 V/cm average voltage, 167% modulation depth, 50 Hz of pulse frequency). DNA was stained with 1 × SYBR Green I, and the result was demonstrated in Fig. 1A. It reveals that PFCE yields better resolution for dsDNA fragments shorter than 7.0 kbp, only if nucleic acid chains between 0.6 and 1.0 kbp migrate together in the matrix, which resisted good resolution. The running buffer for RNA contained 4.0 M urea and 2.0 M acetic acid, respectively. Todorov et al. confirmed that if the urea concentration in the running buffer was above 4.0 M, RNA would be fully denatured and no secondary or tertiary conformations would be present [27,28]. So, prior to separation, RNA was dissolved in 4.0 M urea, heated at 65 °C for 5 min, and then cooled on ice for 3 min to denature. Afterwards RNA samples were introduced into the polymer with 4.0 M urea and 1 × SYBR Green II for separation (Fig. 1B). As described in our previous work [16,29], adding 2.0 M acetic acid into the HEC polymer can realize denaturing during separation, but weaken the fluorescent intensity of the SYBR Green II binding to RNA. Thus, we added 3 × SYBR Green II into the HEC polymer (with 2.0 M acetic acid) to increase the fluorescence signal and the result was demonstrated in Fig. 1C. Data on Fig. 1B and C demonstrate that PFCE yielded a very similar set of resolution for short RNA fragments (<3.0 knt). Moreover, RNA molecule moved faster in HEC with 4.0 M urea (Fig. 1B) than with 2.0 M acetic acid (Fig. 1C). In addition, when the nucleic acid was larger than 1.0 kbp/knt, dsDNA fragment moved faster than the corresponding size of RNA molecule, despite the separation conditions were nearly the same. We tentatively interpret this to the fact that the denaturant strengthens the viscosity of the HEC polymer.

Corresponding to the electropherograms in Fig. 1, Fig. 1D depicts the relative resolution of dsDNA/RNA by PFCE to the one by CE. It shows that the resolution of RNA nearly changes with the same tendency in acetic acid and urea, except in the case of large RNA fragment (>2.0 knt), where the resolution under PFCE seems to deteriorate with the growth of size. However, the resolution of dsDNA by PFCE was improved evidently if its size was above 2.0 kbp. This is possibly the persistence length of dsDNA (50 nm) is longer than RNA (1 nm), inducing large dsDNA fragments to easily aggregate under DC field.

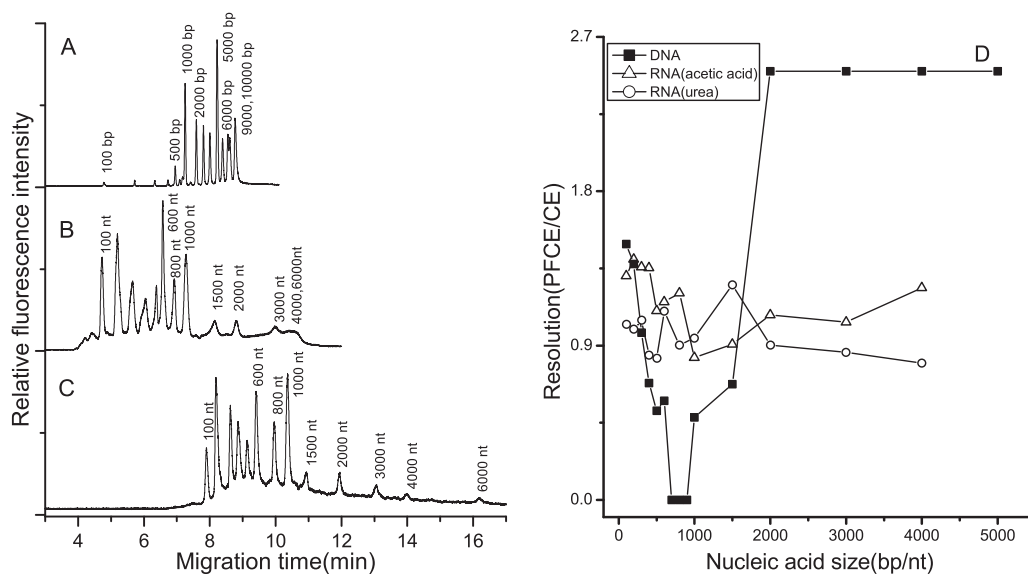


Fig. 1. PFCE electropherograms of the separation of (A) dsDNA; (B) RNA denatured by urea; (C) RNA with denatured by acetic acid; (D) the comparison of resolution of nucleic acid by PFCE with by CE. PFCE was performed at 100 V/cm DC with 167% of modulation depth and 50 Hz of pulse frequency; dsDNA was separated in 0.8% HEC polymer; 4.0 M urea and 2.0 M acetic acid were contained in 0.8% HEC (250 k), respectively. The total length and the effective length of the capillary are 15 cm and 8.0 cm.

3.2. Effect of polymer concentration on nucleic acid migration patterns

Double logarithmic mobility vs. size plot is usually applied to view the migration patterns of nucleic acids [30]. Fig. 2 plots the dependence of electrophoretic mobility of nucleic acids on the concentration of HEC by PFCE with 100 V/cm average electric field strength. It shows that the migration patterns of dsDNA and RNA are significantly different from each other, although the other separation conditions are nearly the same. Analysis reveals (Fig. 2A) that a sigmoidal migration shapes is also observed for dsDNA. The three regimes demonstrated in Fig. 2A are slightly different from the ones described in Ref [20]. In Fig. 2A, small dsDNA fragments (<0.6 kbp) migrate in the Regime I, and calculations indicate that there is a linear relationship between $\log(\text{mobility})$ and size when polymer concentration ranges from 0.4% to 2.0%. Larger ones (>1.0 kbp) migrate in the Regime III. The transition part corresponding to Regime II which looks like a flat line denotes that no separation happens to dsDNA fragments ranging in size from 0.6 to 1.0 kbp. However, this problem could be solved if samples were resolved in a higher mass of HEC (1300 k) at the same concentration [14]. Correspondingly, as shown in Fig. 2B, the transition Regime II disappears, implying that DNA fragments may only proceed by mechanisms related to Regime I and III. This result is probably due to the increase in viscosity caused by the increase of polymer molecular weight. Because the viscosity is dependent on the molecular mass, and two solutions with different molecular mass (polymer type and concentration are the same) will have the same “pore size” as long as they are entangled [31]. Therefore, in PFCE, we suppose that small DNA molecules (<0.6 kbp) migrate in Regime I, which is probably relevant to Ogston sieving, and the rest of the dsDNA ladders (>0.6 kbp) migrate by Regime III, which perhaps relate to the reptation model.

Fig. 2C and D represent the migration trends of RNA with different denaturants in HEC. It shows that the migration patterns of RNA in PFCE are slightly different from the cases under DC conditions [27,32], in which both DNA and RNA demonstrate linear relationship between molecular mass and migration time for nucleic acids smaller than 1000 bases. From the investigation of Fig. 2(C and D), it can be inferred that the electrophoretic mobility (μ) of RNA in

HEC with urea and acetic acid can be expressed as the following equations:

$$\log \mu = A_1 \log N + B_1 \quad (1)$$

$$\log \mu = A_2 (\log N + B_2)^2 + B_3 \quad (2)$$

In this expression, N is the molecule size of nucleic acids. $A_1, A_2, B_1, B_2,$ and B_3 are constants, respectively. The parameters for the regression fits shown in Fig. 2(C and D) are tabulated in Table 1. In all the HEC polymer concentration here, the correlation coefficient R is above 0.99. Eq. (1) shows that the logarithm of mobility linearly decreased with logarithm of RNA size when it was denatured in 4 M urea, Eq. (2) reveals that if RNA is denatured by acetic acid, the log value of mobility declines with the log value of RNA molecule size in parabolic format. The difference between these two migration patterns could possibly be attributed to two reasons. Firstly, as shown in Fig. 1, the peak of RNA fragments is more sharper in sieving polymer containing acetic acid than containing urea as denaturant. This is probably because the secondary and tertiary structures in RNA were thoroughly melted in polymer containing 2.0 M acetic acid [29], indicating that the denaturing ability of 2.0 M acetic was stronger than 4.0 M urea. Secondly, RNA molecules moved slightly slower in the sieving polymer containing acetic acid even though the viscosity for HEC containing 2.0 M acetic (9.84 mPa s) was lower than that of 4.0 M urea (13.8 mPa s).

3.3. Effect of modulation depth on nucleic acid migration patterns

Under conventional DC electrophoresis conditions, the field direction remains unchanged. In square-wave PFCE, the pulse durations are the same for both forward and backward directions, but the value of forward voltage is higher, thus modulation depth and pulse frequency are usually employed to characterize the electric field in PFCE. Visualization experiments [33,34] have demonstrated that these two factors determine the reorientation of nucleic acids in the polymer matrix, and consequently affect the migration

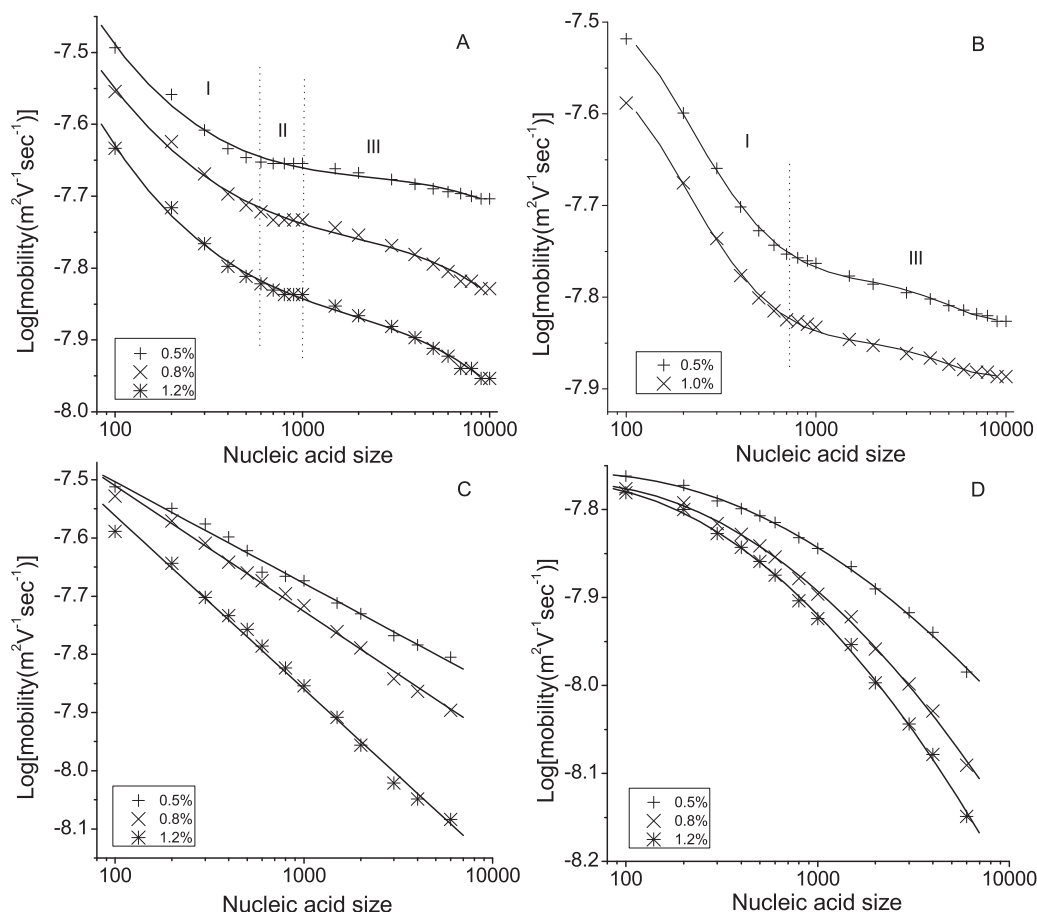


Fig. 2. Dependence of (A) dsDNA (in HEC, 250 k); (B) DNA (in HEC, 1300 k); (C) RNA (urea as denaturant) (in HEC, 250 k); (D) RNA (acetic acid as denaturant) (in HEC, 250 k) mobility on nucleic acid size at different polymer concentrations by PFCE. Other conditions as in Fig. 1.

behavior of nucleic acids in the capillary. Modulation depth scales as

$$\text{Modulation depth (\%)} = 100 \times \frac{(V_f - V_a)}{V_a} \quad (3)$$

where $V_a = (V_f t_f + V_b t_b) / (t_f + t_b)$, V_f and V_b refer to the forward and backward electric potential. t_f and t_b refer to the forward and backward pulse duration time. In order to force the nucleic acids molecules move backward in HEC, the modulation depth should be higher than 100%. Fig. 3 demonstrates the migration patterns of nucleic acids in 0.5% HEC polymer with different modulation depths by PFCE. When modulation depth is above 167% (Fig. 3A), the migration mobility increases with the growth of modulation depth, since the increase of modulation depth enhances Joule heating in capillary, then decreases the viscosity of the polymer [35]. Moreover, the migration trends for DNA are nearly the same. Data on Fig. 3B reveal that in HEC with 4.0 M urea, the migration mobility of RNA varies slightly with the modulation depth. Meanwhile, the linear relationship still holds for the short RNA (<0.4 knt). Fig. 3C plots

the dependence of RNA mobility on molecular size when RNA fragments migrated in 0.8% HEC polymer containing 2.0 M acetic acid. It shows that when modulation depth varies from 150% to 200%, the mobility of RNA decreases with the size of RNA in a parabolic manner. Furthermore, for a certain RNA molecule, its mobility always increases with the growth of the modulation depth.

3.4. Effect of pulse frequency on nucleic acid migration patterns

Fig. 4 represents the mobility as function of the nucleic acid size on a log-log plot for 0.8% HEC. As shown in Fig. 4A, the mobility of dsDNA decreases with the increase of pulse frequency. Interestingly, the mobility difference for the adjacent dsDNA fragments, especially the longer ones, increases with the growth of pulse frequency, indicating that higher pulse frequency is in favor of long DNA fragments separation. However, this is slightly different from our observation in HEC(1300 k) [14], where the mobility reached the minimum at 31.3 Hz. In PFCE, we name the frequency at which the molecular mobility reaches the lowest as resonance frequency.

Table 1

The relationship between RNA mobility (μ) and its size (N) with urea and acetic acid as denaturants, respectively. $A_1, A_2, B_1, B_2,$ and B_3 are constants.

%HEC(w/w)	$\log \mu = A_1 \log N + B_1$			$\log \mu = A_2 (\log N + B_2)^2 + B_3$			
	A_1	B_1	R	A_2	B_2	B_3	R
0.5	-0.1744	-7.1548	0.9954	-0.0540	-1.7519	-7.7587	0.9986
0.8	-0.2159	-7.0787	0.9974	-0.0742	-1.7155	-7.7700	0.9987
1.2	-0.2979	-6.9661	0.9970	-0.0837	-1.6653	-7.7703	0.9987

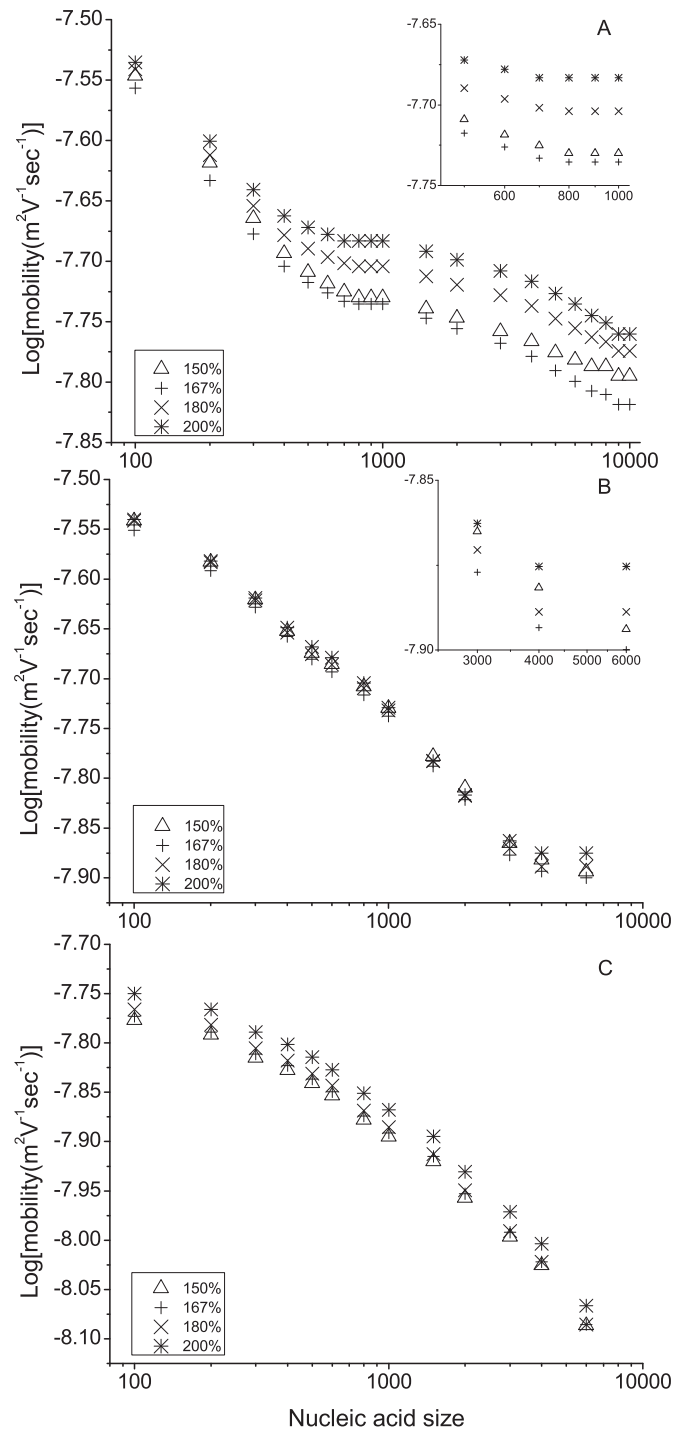


Fig. 3. Dependence of mobility of nucleic acids on chain size at various modulation depths: (A) DNA; (B) RNA denatured in 4.0 M urea; (C) RNA denatured in 2.0 M acetic acid. Other conditions as in Fig. 1.

Such difference indicates that the resonance frequency is probably related to the molecular mass of the polymer, because the molecular mass affects the viscosity of the polymer. Data on Fig. 4B reveal that for different pulse frequencies, RNA fragments migrate at a stable speed in HEC polymer containing 4.0 M urea. Meanwhile, the mobility linearly declines with the molecular size of RNA. For RNA marker in 0.8% HEC polymer with 2.0 M acetic acid (Fig. 4C), the mobility varies with the molecular weight in a parabolic manner, and the mobility reaches the lowest at 12.5 Hz of pulse frequency.

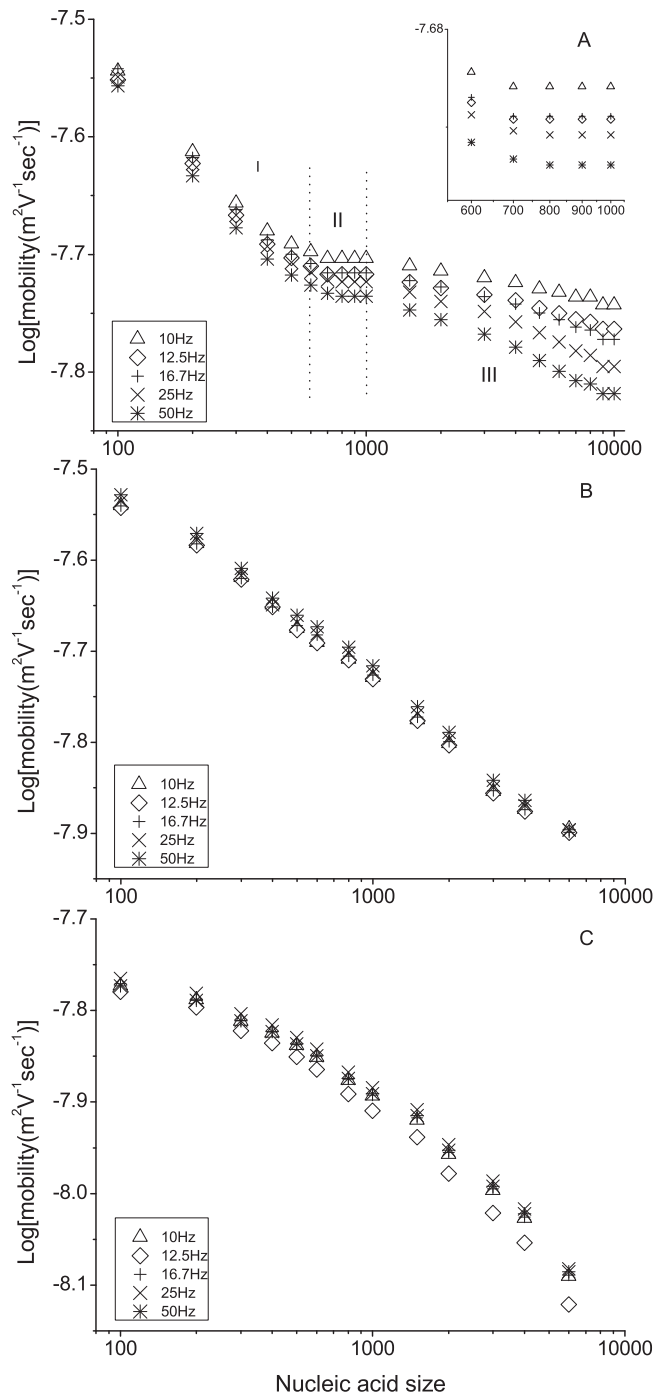


Fig. 4. Dependence of mobility of nucleic acids on chain size at various pulse frequencies: (A) DNA; (B) RNA denatured in 4.0 M urea; (C) RNA denatured in 2.0 M acetic acid. Other conditions as in Fig. 1.

3.5. Short and long nucleic acids migration patterns

In order to make sure the Regime I and III migration patterns of nucleic acids in PFCE, we compared the above results with the predictions from the classical Ogston and reptation models. We have replotted the data at 0.8% HEC, 50 Hz of pulse frequency with different modulation depths by semilogarithmic plot (Fig. 5). In all cases, a linear relationship between log(mobility) and size is present for short dsDNA (<0.3 kbp) and RNA ($N < 0.3$ knt) (4.0 M urea as denaturant). However, using acetic acid as denaturant, linear relationship between log(mobility) and size only appears for high modulation

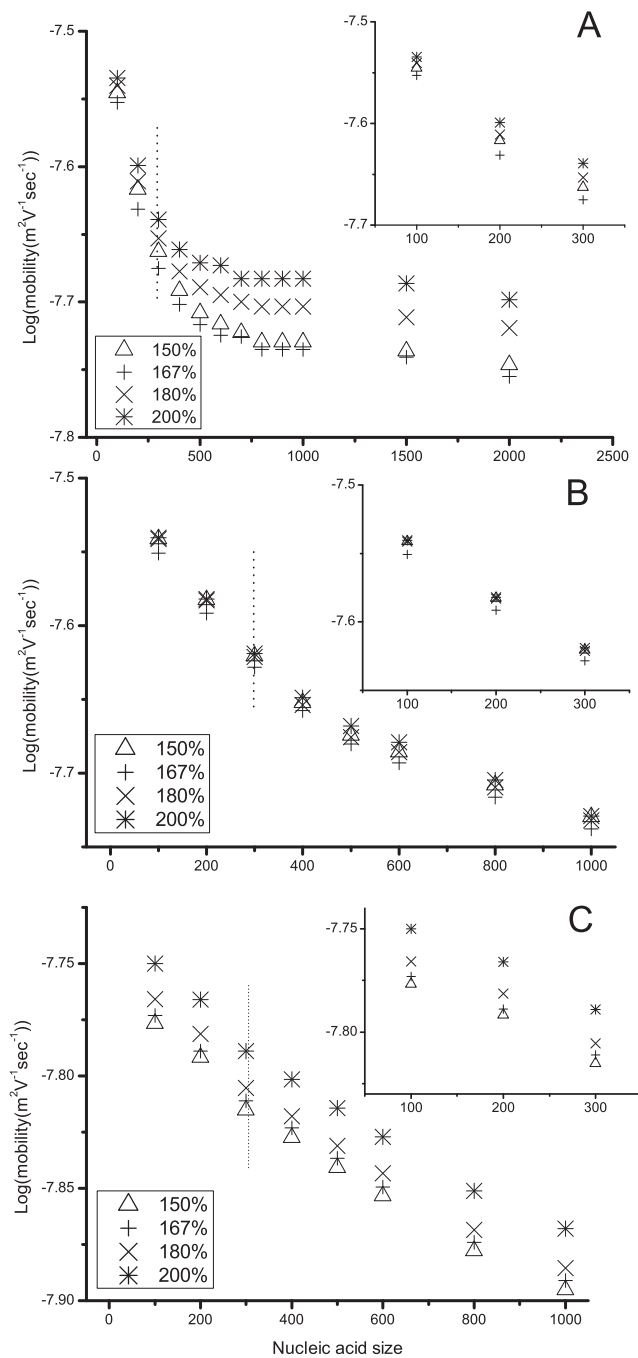


Fig. 5. Semi-log plot of mobility as a function of nucleic acid size at various modulation depths: (A) DNA; (B) RNA denatured in 4.0M urea; (C) RNA denatured in 2.0M acetic acid. Other conditions as in Fig. 1.

depth (>167%). So we suppose that Ogston model may be suitable for dsDNA and RNA (urea as denaturant) in PFCE.

For the long nucleic acids, we introduced “reptation plot” ($3\mu N/\mu_0$ versus N) to further confirm our assumption [36]. $\mu(\text{m}^2\text{V}^{-1}\text{s}^{-1})$ and $\mu_0(\text{m}^2\text{V}^{-1}\text{s}^{-1})$ denote the mobility and the free solution electrophoretic mobility of nucleic acids, respectively. We observe straight lines, converging to one point on the ordinate, for dsDNA chains (>1.5 kbp) (Fig. 6A) and RNA (>0.5 knt) (Fig. 6B) (urea as denaturant), implying that relatively large dsDNA chains and RNA may proceed by reptation model. Furthermore, for the relatively large RNA molecules above 0.5 knt, there is a minor change in slopes at different modulation depths (Fig. 6B), indicating that

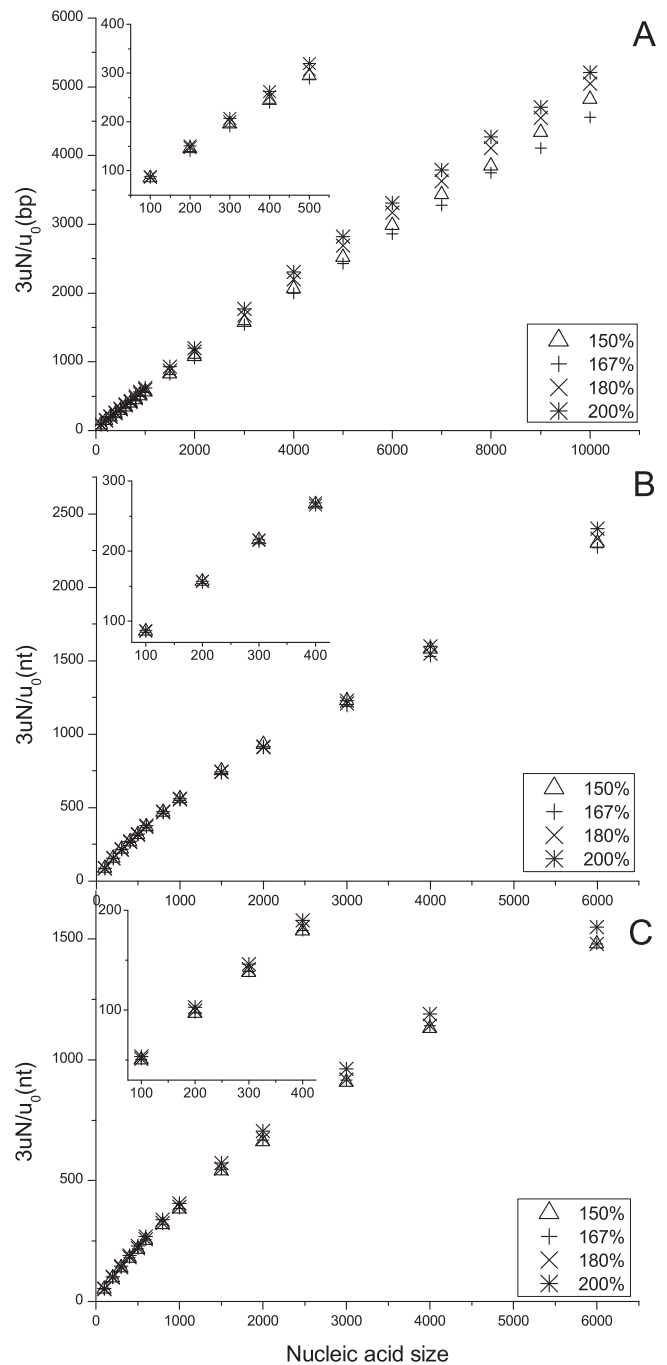


Fig. 6. “Reptation plot” for (A) DNA; (B) RNA denatured in 4.0M urea; (C) RNA denatured in 2.0M acetic acid at various modulation depths. Other conditions as in Fig. 1.

Table 2

The separation voltage for the forward V_f and backward V_b at 1500V of average separation voltage (V_a) and 167% of modulation depth.

V_a (V)	V_f (V)	V_b (V)
500	1335	-335
650	1736	-436
800	2136	-536
950	2537	-637
1100	2937	-737

the RNA molecules above 0.5 knt probably move in reptation without orientation regime under pulsed field conditions. Meanwhile, for dsDNA <1.5 kbp and RNA <0.5 knt, a monotonically increasing mobility function with negative curvature was observed, suggesting that both short dsDNA and RNA (urea as denaturant) proceeded

in Ogston sieving regime, which confirmed our assumption above. As shown in Fig. 6C, although there is a monotonically increasing mobility with negative curvature for RNA in the whole range, a considerable curvature also observed for RNA (>0.6 knt) in the semilogarithmic plot. It can be concluded that Ogston and reptation models are not good descriptions of migration mechanism of RNA (acetic acid as denaturant) in PFCE.

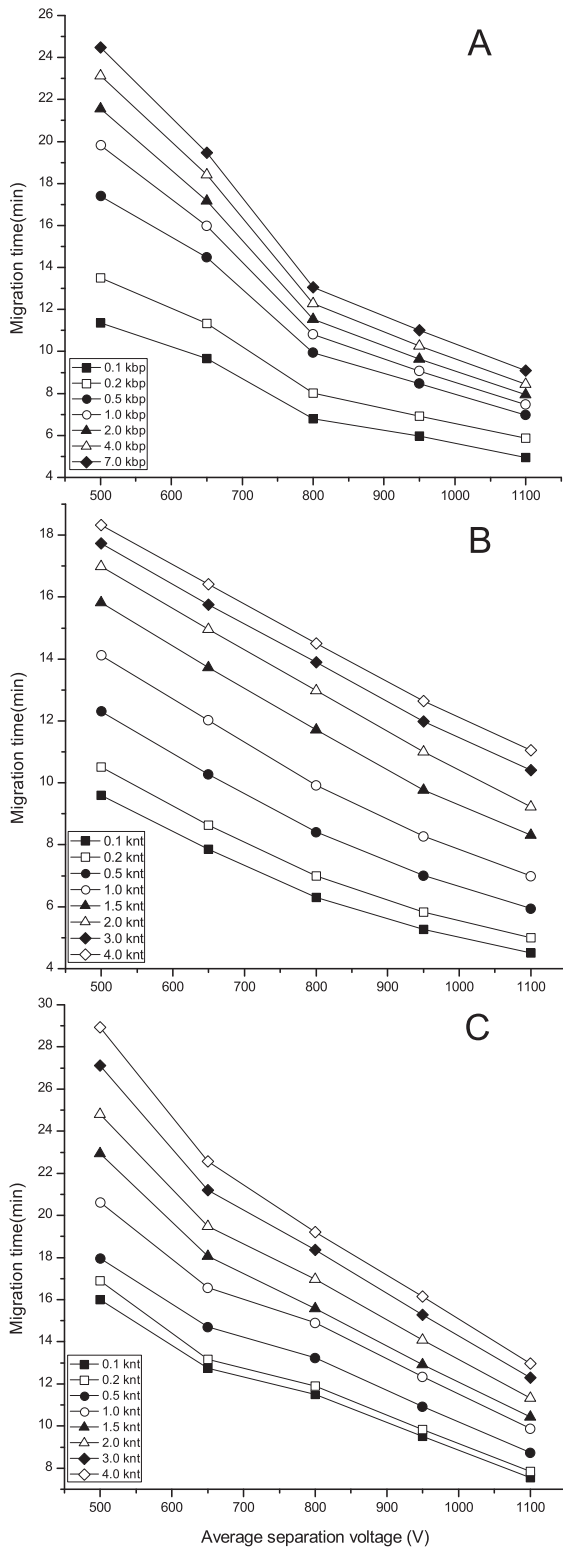


Fig. 7. Dependence of T_m of nucleic acids on average separation voltage: (A) DNA; (B) RNA denatured in 4.0M urea; (C) RNA denatured in 2.0M acetic acid. The total length and effective length of the capillary are 10 cm and 8.0 cm, respectively, other conditions as in Fig. 1.

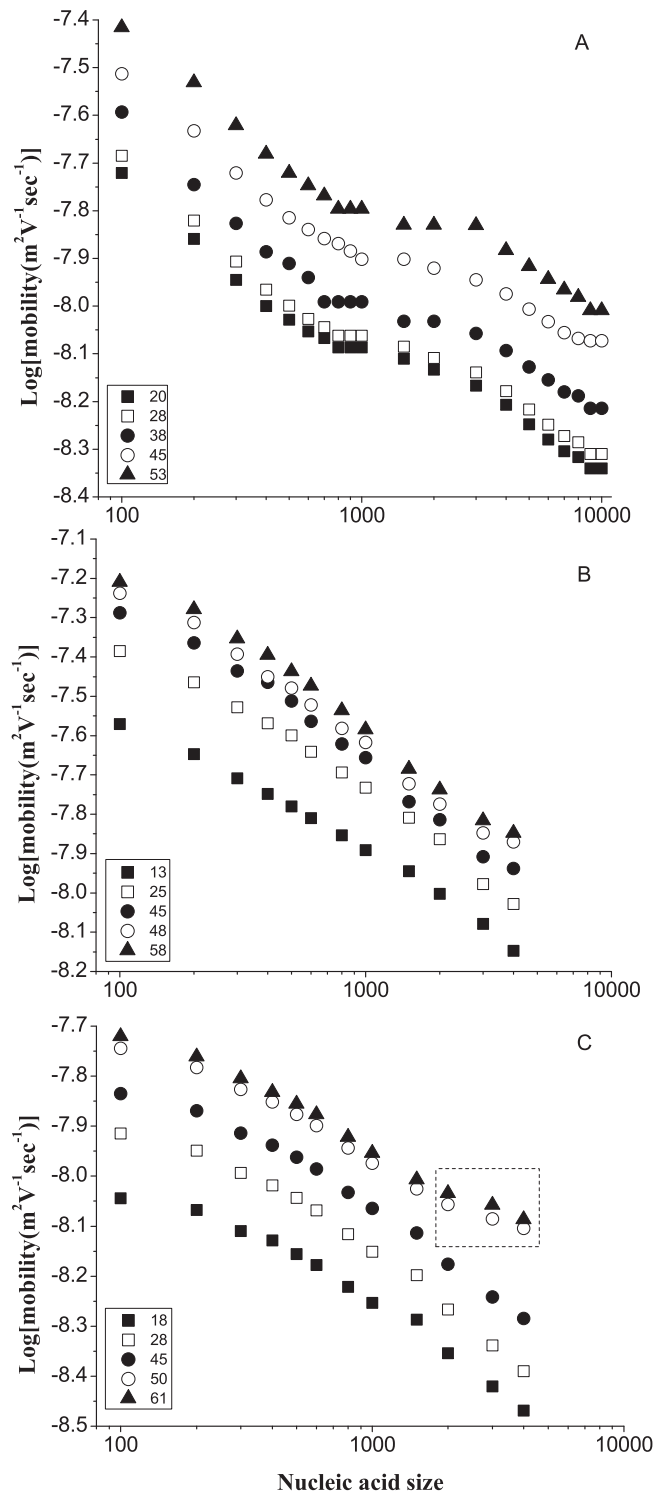


Fig. 8. Dependence of nucleic acids mobility on artificial temperature increase in capillary volume: (A) DNA; (B) RNA denatured in 4.0M urea; (C) RNA denatured in 2.0M acetic acid. Other conditions as in Fig. 1.

3.6. Effect of average separation voltage on T_m of nucleic acids

In CE, when the total length of the capillary is constant, the migration velocity of analytes will be determined by the field force of the nucleic acids. Under pulsed field conditions, the field force was dependent on the average separation voltage (V_a) enforced on the two sides of the capillary. Thus, we have studied the dependence of T_m of nucleic acids on V_a in PFCE. Fig. 7 shows an example of T_m against V_a in 0.8% HEC at 167% modulation depth, 50 Hz squared wave PFCE, and V_a varied from 500 V to 1100 V. Under such pulsed field conditions, V_f and V_b , which was tabulated in (Table 2), can be calculated according to Eq. (3). It shows that T_m of DNA and RNA decreases with the increasing of V_a . Especially for RNA denatured in 4.0 M urea, T_m seems linearly related to V_a . This is mainly caused by two reasons. One is due to the increasing electric force of acetic acid from the growth of average separation voltage V_a . The other reason is ascribed to the decreased viscosity of the polymer that is induced by the joule heating with the growth of electric field.

3.7. Effect of temperature on the mobility of nucleic acids

Temperature is another important factor that may influence the separation performance of nucleic acids by CE [37,38], and there are mainly two factors for temperature increase in the separation polymer. One is joule heating induced by the high voltage, while the other one is caused by the artificial temperature increase in the capillary. Here, we mainly investigated the latter one by enclosing the capillary volume with water at various temperatures ranging from 20 °C to 60 °C. Fig. 8 shows one example of nucleic acids separation in 0.8% HEC at 167% modulation depth, 50 Hz squared wave PFCE, and 100 V/cm of average electric field strength. It shows that under certain PFCE conditions, the mobility of DNA/RNA increases with the growth of temperature. This is most likely caused by the decrease of polymer viscosity as the temperature increases in polymer [37]. Moreover, as shown in Fig. 8, the mobility of DNA displays a zigzag curve (Fig. 8A) with the increase of DNA size. For the case of RNA, its mobility response to the temperature is relatively complicated. If RNA is denatured in 4.0 M urea, its mobility is nearly proportional to its size. However, if RNA is denatured in 2.0 M acetic acid, it migrates in the same parabolic trend at the temperature lower than 45 °C and the RNA fragments above 1.5 knt cannot be clearly resolved at the temperature higher than 45 °C, as marked rectangle with dash line in Fig. 8C. That is understandable when we consider the low viscosity in the polymer at elevated temperature.

4. Concluding remarks

In this work, we have presented a comparative study of RNA and dsDNA electrophoretic migration behavior under different pulsed field conditions. The influence of important parameters on the nucleic acids migration patterns was mainly investigated. Those parameters include polymer concentration, modulation depth, pulse frequency, average separation voltage, and temperature of the capillary volume. Results show that dsDNA and RNA demonstrate significantly different migration patterns. Furthermore, the migration pattern of RNA is related to the denaturant used in PFCE. If the nucleic acids separation mechanisms in CE are still applicable

in PFCE, dsDNA may undergo Ogston, transition regime, and reptation regimes, and RNA proceeds by Ogston and reptation without orientation regimes under pulsed field conditions. Average separation voltage studies suggest that the T_m decreases with the increase of V_a , and the T_m of RNA seems linearly related to the average separation voltage. The mobility of nucleic acids increases with the increment of artificial temperature in the capillary volume. Such a study provides insight into the mechanism of RNA and dsDNA in PFCE and will help optimize nucleic acids separation.

Acknowledgements

We gratefully acknowledge financial support from China Scholarship Council and Consolidated Research Institute for Advanced Science and Medical Care of Waseda University (Japan) (ASMeW). The work was also supported by the National Natural Science Foundation of China (No. 21205078), Research Fund for the Doctoral Program of Higher Education of China (No. 20123120110002).

References

- [1] J.M. Kolesar, P.G. Allen, C.M. Doran, J. Chromatogr. B 697 (1997) 189.
- [2] J.J. Schweinfus, M.D. Morris, Macromolecules 32 (1999) 3678.
- [3] J. Khandurina, H. Chang, B. Wanders, A. Guttman, BioTechniques 32 (2002) 1226.
- [4] L. Ding, X.-X. Zhang, W.-B. Chang, W. Lin, M. Yang, J. Chromatogr. B 814 (2005) 99.
- [5] P. Mikus, K. Marakova, J. Marak, I. Nemeč, I. Valaskova, E. Havranek, Curr. Pharm. Anal. 5 (2009) 171.
- [6] C. Heller, S. Magnúsdóttir, J.-L. Viovy, Methods Mol. Biol. 162 (2001) 293.
- [7] L. Song, M. Maestre, J. Biomol. Struct. Dyn. 9 (1991) 525.
- [8] L. Mitnik, C. Heller, J. Prost, J.L. Viovy, Science 267 (1995) 219.
- [9] G.F. Carle, M.V. Olson, Nucleic Acids Res. 12 (1984) 5647.
- [10] D.C. Schwartz, C.R. Cantor, Cell 37 (1984) 67.
- [11] D. Schoonmaker, T. Heimberger, G. Birkhead, J. Clin. Microbiol. 30 (1992) 1491.
- [12] C. Xu, Q. Liu, B. Diao, B. Kan, X. Song, D. Li, J. Microbiol. Methods 76 (2009) 6.
- [13] D.N. Heiger, A.S. Cohen, B.L. Karger, J. Chromatogr. A (1990) 33, 516.
- [14] Z. Li, X. Dou, Y. Ni, K. Sumitomo, Y. Yamaguchi, J. Sep. Sci. 33 (2010) 2811.
- [15] Z. Li, X. Dou, Y. Ni, Y. Yamaguchi, Anal. Bioanal. Chem. 401 (2011) 1665.
- [16] Z. Li, X. Dou, Y. Ni, K. Sumitomo, Y. Yamaguchi, Electrophoresis 31 (2010) 3531.
- [17] Z. Li, X. Dou, Y. Ni, Q. Chen, S. Cheng, Y. Yamaguchi, J. Chromatogr. A (2012) 274, 122.
- [18] J.L. Viovy, Rev. Mod. Phys. 72 (2000) 813.
- [19] G.W. Slater, C. Desruisseaux, S.J. Hubert, J.-F. Mercier, J. Labrie, J. Boileau, F. Tessier, M.P. Pépin, Electrophoresis 21 (2000) 3873.
- [20] T.I. Todorov, M.D. Morris, Electrophoresis 23 (2002) 1033.
- [21] M.N. Albarghouthi, A.E. Barron, Electrophoresis 21 (2000) 4096.
- [22] J.-L. Viovy, T. Duke, Electrophoresis 14 (1993) 322.
- [23] A.G. Ogston, Trans. Faraday Soc. 54 (1958) 1754.
- [24] G.W. Slater, J. Noolandi, Phys. Rev. Lett. 55 (1985) 1579.
- [25] D. Schmalzing, C.A. Piggee, F. Foret, E. Carrilho, B.L. Karger, J. Chromatogr. A 652 (1993) 149.
- [26] S. Hjertén, J. Chromatogr. A (1985) 191, 347.
- [27] T.I. Todorov, O. de Carmejane, N.G. Walter, M.D. Morris, Electrophoresis 22 (2001) 2442.
- [28] T.I. Todorov, Y. Yamaguchi, M.D. Morris, Anal. Chem. 75 (2003) 1837.
- [29] K. Sumitomo, M. Sasaki, Y. Yamaguchi, Electrophoresis 30 (2009) 1538.
- [30] V. Dolník, W.A. Gurske, Electrophoresis 20 (1999) 3373.
- [31] C. Heller, Electrophoresis 22 (2001) 629.
- [32] J. Skeidsvoll, P.M. Ueland, Electrophoresis 17 (1996) 1512.
- [33] X. Shi, R.W. Hammond, M.D. Morris, Anal. Chem. 67 (1995) 1132.
- [34] X. Shi, R.W. Hammond, M.D. Morris, Anal. Chem. 67 (1995) 3219.
- [35] Y. Kim, E.S. Yeung, Electrophoresis 18 (1997) 2901.
- [36] G.W. Slater, in: C. Heller (Ed.), Analysis of Nucleic Acids by Capillary Electrophoresis, Vieweg und Sohn, Wiesbaden, 1997.
- [37] B. Siles, D. Anderson, N. Buchanan, M. Warder, Electrophoresis 18 (1997) 1980.
- [38] J. Knox, K. McCormack, Chromatographia 38 (1994) 207.